International Journal of Engineering &Technology, 8 (3) (2019) 162-168

International Journal of Engineering & Technology

Website: www.sciencepubco.com/index.php/IJET

Research paper

Development of antipodal Vivaldi antenna for microwave brain stroke imaging system

Azahari Salleh [1, 2], Ching Chiou Yang [1], Mandeep Singh Jit Singh [1], Mohammad Tariqul Islam [1] *

[1] Centre of Advanced Electronic and Communication Engineering (PAKET), Faculty of Engineering and Built Environment, Universiti Kebangsaan Malaysia, 43600, UKM, Bangi, Selangor, Malaysia
[2] Centre for Telecommunication Research & Innovation (CeTRI), Fakulti Kejuruteraan Elektronik dan Kejuruteraan Komputer (FKEKK), Universiti Teknikal Malaysia Melaka, Hang Tuah Jaya, 76100, Durian Tunggal, Melaka
**Corresponding author E-mail: azahari@utem.edu.my*

Abstract

In recent years, Microwave Imaging (MWI) has offered an effective solution in medical applications, especially in detecting abnormal body tissues in the human brain. Among the popular detection methods currently being used in hospitals are Magnetic Resonance Imaging (MRI) and Computed Tomography (CT) scans. But the constraints faced by this method include the high cost of equipment and its large size and static nature. In this article, the antipodal Vivaldi antenna for the microwave brain stroke imaging system is designed and presented. Nine antipodal Vivaldi antennas were proposed and designed using Computer Simulation Technology (CST) software operating from 2.06 GHz to 2.61 GHz. A Radio Frequency (RF) switch was used to enable the antenna sequentially received the backscattered signal from the head phantom. Then, MATLAB software was used to interface between the Python algorithm and the Vector Network Analyzer (VNA) for the purpose of data collection. The Python algorithm was able to control the rotation of the platform, which rotated in 50 positions. The fabricated antennas are based on a Rogers RO4350B substrate and show good agreement between the measured result and simulated result. The designed antennas were able to achieve 86.92% average efficiency, 2.45 dBi gain and stable radiation directivity. Finally, from the variation of the color in color plot, a target structure was successfully detected.

Keywords: *Antipodal Vivaldi Antenna; Brain Stroke; Computer Simulation Technology; Microwave Imaging System; Matlab.*

1. Introduction

Microwave imaging (MWI) systems have been broadly utilized in numerous application such as materials characterization, medical application and remote sensing [1]–[3]. This innovation has been applied to detect unusual tissues in the brain stroke and breast cancer [4], [5]. The ability to penetrate into the dielectric material through microwave frequencies, has enabled MWI to be widely used primarily in abnormal body tissue detection in the human body. The human body is dielectric material with dielectric properties of permittivity is between 56.5 - 42.8 [6]. This system operates using an antenna that produces electromagnetic energy in microwave frequencies. In MWI, a system antenna is used as transmitter and receiver. For signal transmission, microwave signals are transmitted from the antenna to the imaging object. The signal penetrates through the imaging object and is collected by the receiving antenna. The target image is obtained after the backscattered signal of the object is measured and processed [7]. Numerous research that has been conducted around the world on designing a MWI system for detecting breast cancer [5], [8]–[10] and human head imaging [11]–[15].

Major brain stroke can be classified into ischemic stroke and hemorrhagic stroke. Ischemic stroke occurs when a blood vessel becomes blocked or narrowed by a blood clot causing oxygen stops flows to the brain to cease stopping functioning. Hemorrhagic stroke occurs when a blood vessel burst and spills blood into the brain and causing the surrounding tissue stop functioning [16]. Present devices for brain stroke detection include the CT scan, MRI, X-ray mammograms, and ultrasound [17]. MRI and CT are very effective diagnosis tools, but they are very expensive. In fact, most hospitals are unable to afford reliable diagnosis tools [18]. Diagnosis tools are also, bulky, not portable and require a large space for system setup [19]. The primary disadvantage of the CT scan is that it produces excessive radiation effect (effective dose is approximately 5 mSv), while MRI is more complex and takes a long time to complete an examination [20].

Basically, the development of MWI system for the human phantom consists of three important elements: the development of rotation platforms, antenna and data acquisition for system validation. In this paper, the design of an antenna for microwave brain stroke imaging system is shown in detail, including antenna specifications, simulation and fabrication of antenna and testing the antenna for microwave brain stroke imaging system. For verification, two sets of reflection coefficient were collected around the head phantom, consisting of one with target structure and one without a target structure.

2. Antenna configuration

In MWI system, an antenna with a directional radiation pattern and wide bandwidth the important factors in medical applications [21]–[23]. A directional antipodal Vivaldi antenna is proposed due to the compact size, low cost, easy to fabricate, high gain and directive radiation is suitable to form an antenna array around the head phantom for data acquisition [24]–[26]. The antenna operates over the band 2.06 GHz – 2.61GHz. This frequency range gives a reasonable compromise between the desired signal penetration and acceptable image resolution [17], [27]. The exponential profile curves of the antenna provide better performance than the parabola and trigonometric functions.

An antipodal Vivaldi antenna consists of two sides and radiating structure is in the form of two exponentially tapered arms. One side of the antenna is printed on the top and another tapered in the opposite direction is printed on the bottom of the dielectric material. The antipodal Vivaldi antenna is very difficult to analyse because of the transmission constant of the tapered slot and characteristic impedance. Therefore, the antenna was designed through the simulation calculation and optimized using genetic algorithm in the CST software. The antenna is printed on the substrate of Rogers RO4350B with a thickness of 1.524 mm, dielectric constant of 3.48 and loss tangent of 0.0039 which is relatively small compared to other substrates. The overall size of the antenna is 50 mm length x 60 mm width and the fabricated antennas shown in Figure 1. Table 1 shown the design specification of the proposed antenna.

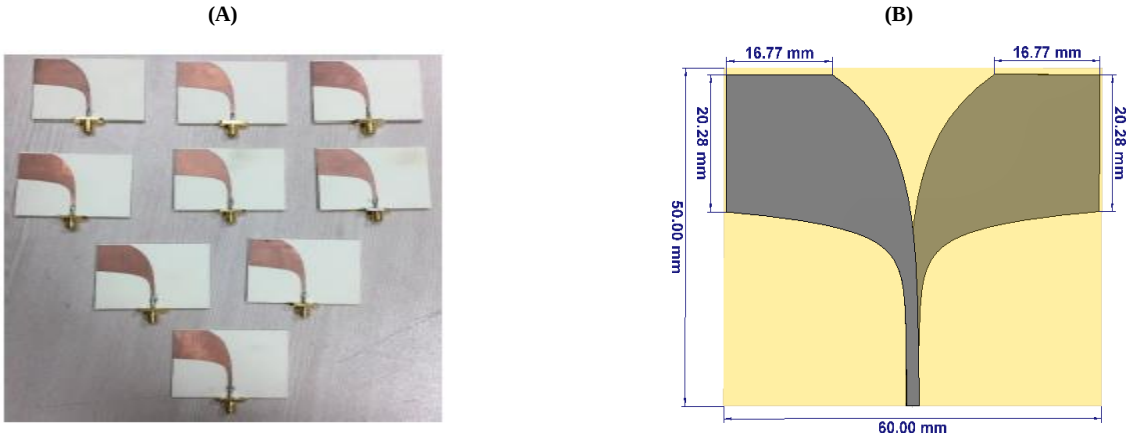

Fig. 1: (A) Antenna Dimension; (B) Fabricated Antenna.

Table 1: Antenna Specifications

Antenna Characteristic	Value
Operating Frequency	2.06 – 2.61 GHz
Operating Bandwidth	550 MHz
Substrate Dielectric	3.48
Substrate Loss Tangent	0.0039
Average Gain	2.45 dB
Average Efficiency	86.92%
Input Impedance	50 Ω
Radiation Pattern	Directional

The system used the mono-static radar mode of operation. In mono-static mode, one antenna was applied as the transmitter and other eight antennas were applied as the receiver. An Agilent N5227A Vector Network Analyzer (VNA) used to generate and receive the microwave signal. The transmitting antenna was connected to the port 1 of the VNA and other eight antennas were connected to the RF switch, while the output of the RF switch was connected directly to the port 2 of the VNA.

3. Result and discussion

The CST software is used for the antenna simulation. The Agilent E8362C vector network analyzer and Satimo near field measurement lab (UKM StarLab) were used to obtain the measured results of the antenna. The measurement setup is shown in Figure 2. The Agilent E8362C VNA was able to covers the range of the frequency from 10 MHz to 67 GHz using the SatEnv software and Satimo Passive Measurement (SPM). The measured results and the simulated results have been plotted using the data analysis Origin Pro 9.0 software for the purpose of comparison.

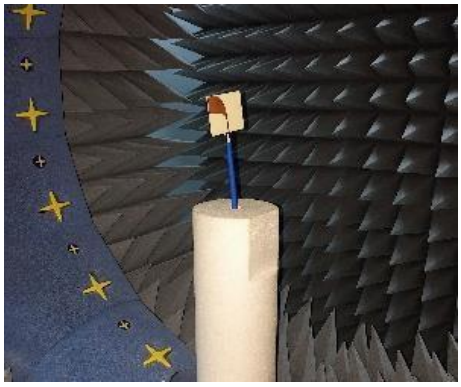

Fig. 2: Antenna Measurement Setup at Satimo Lab.

Figure 3 shows the simulated and measured reflection coefficient (S_{11}) of the antenna. The result indicate that the antenna has a reflection coefficient of less than -10 dB across the utilized band. S_{11} less than -10 dB means that at least 90% input power is delivered, and reflected power is less than 10%. The antenna operates over the frequency range from 2.06 GHz – 2.61 GHz and operation bandwidth are approximately 550 MHz by referred to -10 dB reflection coefficient. The measured and simulated results have very good agreement.

Figure 4 illustrates the simulated and the measured Voltage Standing Wave Ratio (VSWR) of the antenna. VSWR measure how well matched the antenna to the feed line. A VSWR value under two is considered a good match with the feed line and suitable for most antenna application. The results show that antenna is matched with the transmission line which is the RF cable because the impedance of the SMA connector that solder at the antenna is 50 Ω which is matched with the characteristics impedance of the RF cable.

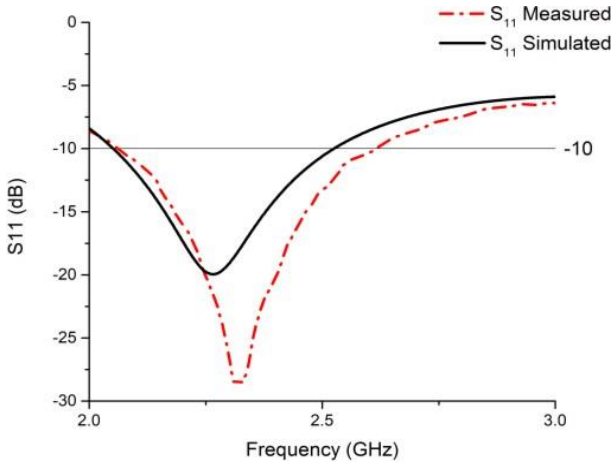

Fig. 3: Reflection Coefficient of Antenna.

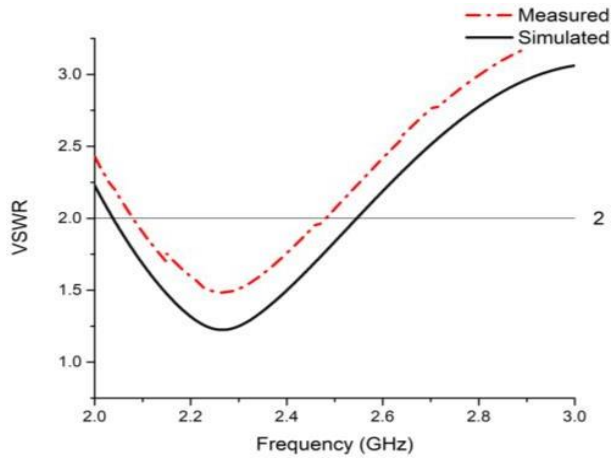

Fig. 4: VWSR of Antenna.

The simulated and the measured efficiency results obtained from the CST microwave Studio and Satimo near field measurement lab were converted into percentage and plotted as shown in Figure 5. The measured average radiation efficiency was approximately 86.92% but the simulated average radiation efficiency was 87.34%. Again, both results are in good agreement. The high efficiency of the antenna indicated that most of the power radiated by the antenna. For low efficiency antenna indicated that most of the power absorbed by the antenna was due to impedance mismatch.

The 2D measured radiation pattern is shown in Figure 6. The cross polar (Phi = 0°), co polar (Phi = 90°) and cross polar (Phi = 90°), co polar (Phi = 0°) are plotted. During the cross polarization the antenna radiation is horizontally polarized and received by the vertically polarized antenna. Cross polarization is always perpendicular to the desired polarization direction. For co- polarization, the antenna is always faced directly to the desired polarization direction. The ideal cross polarization level must be zero or as low as possible but the co polarization must be higher than -10 dB. From the measured results co- and cross polarization meet the requirements.

The simulated 3D radiation pattern at 2.3 GHz indicates the directional radiation, as shown in Figure 7. The result show that the antenna has achieved stable radiation directivity. This ensures that the antenna is able to receive a high range of backscattered signal with the minimum of unwanted noise.

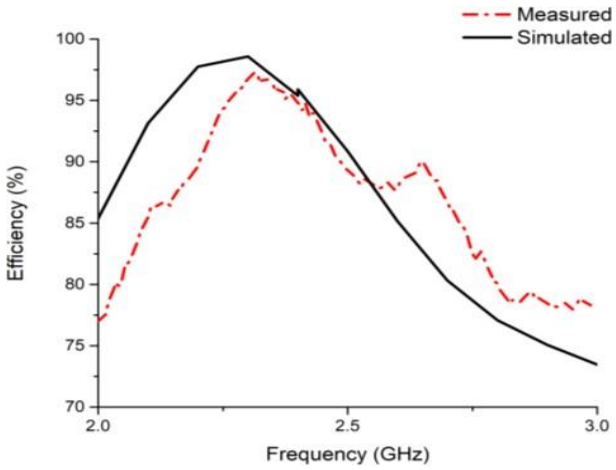

Fig. 5: Efficiency of Antenna.

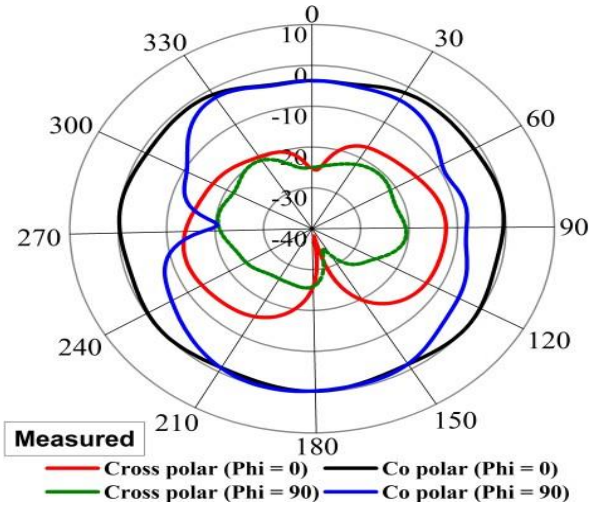

Fig. 6: 2D Radiation Pattern.

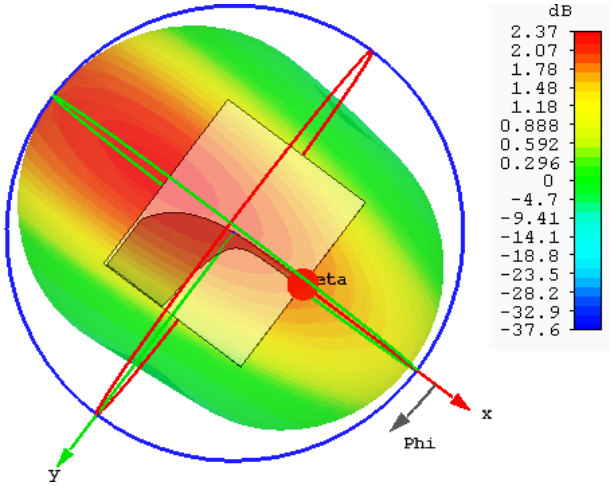

Fig. 7: 3D Radiation Pattern.

After verifying the performance of the antenna, it was mounted at the head imaging rotation platform. The experiment was performed by collected the signal from the head phantom with and without inserted the target structure for the validation purpose. The target structure is the fabricated white matter, which is the main tissues found in the human brain as shown in Figure 8. The white matter was fabricated using water, corn flour, gelatin and sodium azide. Figure 9(a) shown the colour plot of the data using MATLAB that without the target structure and Figure 9(b) with superimposed the target structure. The step frequency from 90 – 150, yellow colour in the colour plot indicated that the transmitted power was absorb by the white matter (due to the lossy brain tissue) and only small amount of radiated power is scattered back receive by the antenna. The colour variation with and without the target structure includes sensible precision and high resolution. Hence, the target structure was successfully detected.

Fig. 8: Fabricated White Matter.

(A)

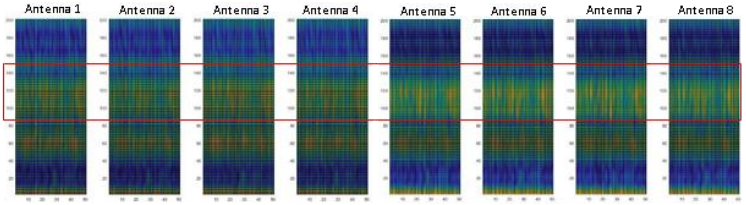

(B)

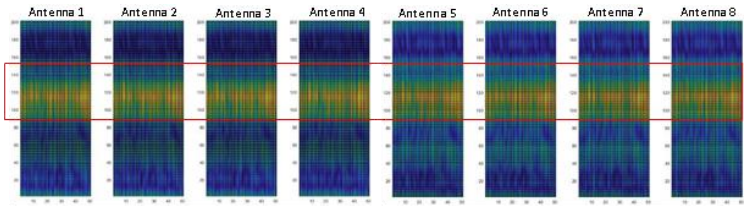

Fig. 9: Color Plot of Data (A) Head Phantom without the Target Structure (B) Head Phantom with the Target Structure.

4. Conclusion

An antipodal Vivaldi antenna was successfully designed and implemented in a microwave brain stroke imaging system. At the initial stage, the antenna was able differentiated target structure of brain stroke at the frequency from 2.06 GHz to 2.61 GHz. There is some room for improvement in term of size, bandwidth and directivity of the antenna which is the big challenges to MWI system. In terms of overall system, the real image of stroke will be fully visualized after implementation of image reconstruction algorithm based on current data.

Acknowledgement

The author would like to thank to Ministry of Education Malaysia and Universiti Teknikal Malaysia Melaka for the scholarship support. This research was funded by Universiti Kebangsaan Malaysia under grant number DIP-2017-014.

References

[1] M. Benedetti, M. Donelli, a. Massa, and a. Rosani, "An innovative microwave imaging technique for non destructive evaluation: applications to civil structures monitoring and biological bodies inspection," *2004 IEEE Int. Work. Imaging Syst. Tech. (IEEE Cat. No.04EX896)*, vol. 55, no. 6, (2004) pp. 1878–1884.
[2] M. Donelli, "Microwave Imaging," in *Imaging with Electromagnetic Spectrum*, Springer, (2014). https://doi.org/10.1007/978-3-642-54888-8_9.
[3] N. K. Nikolova, *Introduction to microwave imaging*. Cambridge University Press, (2017). https://doi.org/10.1017/9781316084267.
[4] A. T. Mobashsher and A. M. Abbosh, "On-site Rapid Diagnosis of Intracranial Hematoma using Portable Multi-slice Microwave Imaging System," *Sci. Rep.*, vol. 6, (2016), 37620. https://doi.org/10.1038/srep37620.
[5] L. Wang, "Microwave Sensors for Breast Cancer Detection," *Sensors*, vol. 18, no. 2, (2018) p. 655. https://doi.org/10.3390/s18020655.
[6] A. T. Mobashsher and A. M. Abbosh, "Artificial human phantoms: Human proxy in testing microwave apparatuses that have electromagnetic interaction with the human body," *IEEE Microw. Mag.*, vol. 16, no. 6, (2015) pp. 42–62. https://doi.org/10.1109/MMM.2015.2419772.
[7] A. T. Mobashsher and A. Abbosh, "Microwave imaging system to provide portable-low-powered medical facility for the detection of intracranial hemorrhage,"*1st Australian Microwave Symposium, Conference Proceedings* (2014), pp. 23–24, https://doi.org/10.1109/AUSMS.2014.7017347.
[8] M. A. Yarlequé Medina and A. Villavicencio Paz, "Microwave Imaging for Breast Cancer Detection : Experimental comparison of Confocal and Holography Algorithms," *IEEE ADESCON* (2016), pp. 0–3, 10.1109/ANDESCON.2016.7836226.
[9] M. T. Islam, M. Z. Mahmud, N. Misran, J. I. Takada, and M. Cho, "Microwave Breast Phantom Measurement System with Compact Side Slotted Directional Antenna," *IEEE Access*, vol. 5, no. c, pp. 5321–5330, 2017. https://doi.org/10.1109/ACCESS.2017.2690671.
[10] A. Rahman, M. T. Islam, M. J. Singh, S. Kibria, and M. Akhtaruzzaman, "Electromagnetic Performances Analysis of an Ultra-wideband and Flexible Material Antenna in Microwave Breast Imaging: To Implement A Wearable Medical Bra," *Sci. Rep.*, vol. 6,(2016), pp. 1–11. https://doi.org/10.1038/srep38906.
[11] M. Persson *et al.*, "Microwave-based stroke diagnosis making global prehospital thrombolytic treatment possible," *IEEE Trans. Biomed. Eng.*, vol. 61, no. 11, (2014), pp. 2806–2817. https://doi.org/10.1109/TBME.2014.2330554.
[12] B. J. Mohammed, A. M. Abbosh, S. Mustafa, and D. Ireland, "Microwave system for head imaging," *IEEE Trans. Instrum. Meas.*, vol. 63, no. 1, (2014), pp. 117–123. https://doi.org/10.1109/TIM.2013.2277562.
[13] P. Tournier *et al.*, "Microwave Tomography for Brain Stroke Imaging," *IEEE International Symposium on Antennas and Propagation & USNC/URSI National Radio Science Meeting*, (2017), pp. 29–30, 10.1109/APUSNCURSINRSM.2017.8072057.
[14] M. Rashed, I. Faruque, M. T. Islam, and N. Misran, "Effect of Human Head Shapes for Mobile Phone Exposure on Electromagnetic Absorption," *Inf. MIDEM*, vol. 40, no. 3, pp. 232–237, 2010.
[15] M. T. Islam and M. R. I. Faruque, "Reduction of Specific Absorption Rate (SAR) in The Human Head with Ferrite Material and Metamaterial," *Prog. Electromagn. Res. C*, vol. 9, pp. 47–58, 2009. https://doi.org/10.2528/PIERC09062303.
[16] N. A.M., "Intracranial hemorrhage," *Am. J. Respir. Crit. Care Med.*, vol. 184, no. 9, (2011), pp. 998–1006. https://doi.org/10.1164/rccm.201103-0475CI.
[17] D. Ireland and M. Bialkowski, "Microwave Head Imaging for Stroke Detection," *Prog. Electromagn. Res. M*, vol. 21, (2011), pp. 163–175. https://doi.org/10.2528/PIERM11082907.
[18] A. T. Mobashsher, K. S. Bialkowski, A. M. Abbosh, and S. Crozier, "Design and experimental evaluation of a non-invasive microwave head imaging system for intracranial haemorrhage detection," *PLoS One*, vol. 11, no. 4, (2016), pp. 1–29. https://doi.org/10.1371/journal.pone.0152351.
[19] A. T. Mobashsher, A. Mahmoud, and A. M. Abbosh, "Portable Wideband Microwave Imaging System for Intracranial Hemorrhage Detection Using Improved Back-projection Algorithm with Model of Effective Head Permittivity," *Sci. Rep.*, vol. 6, (2016), no.20459. https://doi.org/10.1038/srep20459.
[20] J. Vymazal, A. M. Rulseh, J. Keller, and L. Janouskova, "Comparison of CT and MR imaging in ischemic stroke," *Insights into Imaging*, vol. 3, no. 6. (2012), pp. 619–627. https://doi.org/10.1007/s13244-012-0185-9.
[21] M. M. Islam, M. T. Islam, M. R. I. Faruque, M. Samsuzzaman, N. Misran, and H. Arshad, "Microwave imaging sensor using compact metamaterial UWB antenna with a high correlation factor," *Materials (Basel).*, vol. 8, no. 8, (2015), pp. 4631–4651. https://doi.org/10.3390/ma8084631.
[22] H. Yu, G. Yang, Q. Wu, and M. Su, "Design and Optimization of UWB Vivaldi Antenna for Brain Tumor Detection," *IEEE International Conference on Microwave and Millimeter Wave Technology (ICMMT)*, (2016), pp. 2–4 https://doi.org/10.1109/ICMMT.2016.7762401.
[23] A. T. Mobashsher and A. M. Abbosh, "Performance of directional and omnidirectional antennas in wideband head imaging," *IEEE Antennas Wirel. Propag. Lett.*, vol. 15, (2016), pp. 1618–1621. https://doi.org/10.1109/LAWP.2016.2519527.
[24] M. Amiri, F. Tofigh, A. Ghafoorzadeh-Yazdi, and M. Abolhasan, "Exponential Antipodal Vivaldi Antenna with Exponential Dielectric Lens," *IEEE Antennas Wirel. Propag. Lett.*, vol. 16, (2017), pp. 1792–1795. https://doi.org/10.1109/LAWP.2017.2679125.

[25] G. Veerendra Nath, K. Nageswara Rao, and K. Hari Kishore, "A slot loaded compact antipodal vivaldi antenna design for RADAR applications," *J. Adv. Res. Dyn. Control Syst.*, vol. 10, no. 7, (2018), pp. 1342–1346. https://doi.org/10.14419/ijet.v7i2.8.10325.

[26] N. Ardelina, E. Setijadi, P. H. Mukti, and B. Manhaval, "Comparison of array configuration for Antipodal Vivaldi antenna," in *Proceeding - 2015 International Conference on Radar, Antenna, Microwave, Electronics, and Telecommunications, ICRAMET 2015*, (2015), pp. 40–45, 10.1109/ICRAMET.2015.7380771 https://doi.org/10.1109/ICRAMET.2015.7380771.

[27] D.-C. Chang, L.-D. Fang, W.-H. Fang, and C.-H. Lee, "Tradeoff study of microwave imaging for biomedical application," *2013 IEEE MTT-S Int. Microw. Work. Ser. RF Wirel. Technol. Biomed. Healthc. Appl.*, (2013), pp. 1–3, 10.1109/IMWS-BIO.2013.6756257. https://doi.org/10.1109/IMWS-BIO.2013.6756257.